

# Adaptive Optics based Telescope Arrays Receiver for Compensation of Optical Turbulence Effects in a Deep-Space Optical Communication link with Mars

A. Hashmi<sup>1</sup>, Member, IEEE, A. Eftekhar<sup>1</sup>, A. Adibi<sup>1</sup>, and F. Amoozegar<sup>2</sup>

**Abstract**—Future deep-space exploration missions demand a broadband and integrated communication infrastructure to transport the scientific data to Earth. Optical communication employing optical arrays receiver is a viable alternative to the current NASA deep-space RF-based network. Atmospheric turbulence is a major limiting factor for the inter-planetary optical links. Investigation of the use of adaptive optics subsystems is carried out for the compensation of coupled effects of optical turbulence and background noise, in direct detection optical array receivers. The simulation and analysis of an end-to-end deep-space optical communication link between a spacecraft in Mars orbit and Earth-based telescope array receivers show that the incorporation of adaptive optics systems results in considerable performance improvement in achievable data rates.

**Index Terms**— Adaptive optics, array signal processing, extra-terrestrial exploration, optical communication, satellite communication.

## I. INTRODUCTION

THE international scientific community and NASA continue to send discovery missions in space to unravel the mysteries of deep-space planets in the solar system, galaxies, and the universe. A high bit-rate, integrated, standardized, and reliable communication link is required between a spacecraft in deep-space and a receiver at Earth to transport large volumes of scientific data [1].

NASA's deep-space ventures so far have relied upon a global RF-based deep-space network (DSN) to capture the signal returns from the planets. The DSN uses X-band and more recently, Ka-band capabilities have been successfully tested [2]. The current RF technology has reached an extremely high limit of performance, since the spacecraft antenna sizes and transmitter powers are already at maximum feasible limit. On Earth, DSN receiving antennas are enormous (34-m and 70-m diameters), and the receiving systems are already operating at just a few degrees above absolute zero [3]. The current data rates are limited to just hundreds of kilobits per second (Kbps) range from Mars

farthest distances [4], and lower data rates for outer planets.

As compared to RF technology, optical communications technology has the added advantages of higher gain smaller diameter antennas, a higher center frequency for extremely fast modulations, and a larger available spectrum. Hence, optical communication systems show promising prospects for the deep-space communication. The need for deep-space optical communications has been articulated in the NASA 2003 Strategic Plan [3, 5] as a “New Effort Building Block” under the “Communications Technological Barrier” for “providing efficient data transfer across the solar system.” In this effort, NASA announced the launch of a Mars Laser Communication Demonstration (MLCD) platform to test the first-ever interplanetary laser-communication link between Earth and Mars in 2009-2011 time-frame [6, 7].

The initial analysis has shown that a large aperture telescope (at least 10- m diameter) is required to obtain the acceptable bit-rates (in M bps range) for a communication link between Earth and Mars [8, 9]. A single large telescope has the limitations of high cost, single point failure in case of malfunction, and difficulty to attain the diffraction-limited performance. An array of relatively smaller size telescopes is a viable alternative. Telescope arrays have advantages of lesser cost, improved diffraction-limited performance, slighter gravitational effects, scalability, and redundancy in operations [10,11]. It has been shown that for ground-based direct detection reception, telescope arrays can approach the same performance as that of a large monolithic telescope having the same total photons collecting area [10,11].

Atmospheric turbulence is a major limiting factor in a free-space optical communication link. Optical turbulence distorts the phase of the propagating optical fields and limits the focusing capabilities of the telescope antennas [12]. In the presence of optical turbulence, the focal spot size is dependent upon the atmospheric Fried parameter. The turbulence limited spot size is much greater than the ideal diffraction-limited one. Hence, a larger detector is required to encompass the signal energy in the focal-plane. In a typical deep-space optical communication link, some background light (from Sun, sky etc.) always enters the receiver field-of-view (FOV) along with the desired signal light fields [13]. As we increase the detector dimensions to capture the widespread signal energy, the number of background photons received also increases. This results in the degradation of the overall signal to background noise photons ratio, and performance of the

<sup>1</sup> Authors are with School of ECE at Georgia Institute of Technology, Atlanta, GA 30332 USA. (Corresponding author, A. Hashmi : 404-324-3385; fax: 404-894-4641; e-mail: hashmi@ece.gatech.edu).

<sup>2</sup> Author is with Jet Propulsion Laboratory (NASA), California Institute of Technology, Pasadena, California 91109 USA. (email: Farid.Amoozegar@jpl.nasa.gov).

optical receiver. Unfortunately, both the atmospheric turbulence and background noise are at their respective peaks during the daytime, and mitigation of these effects is the foremost challenge.

In this paper, we analyze the use of adaptive optics (AO) subsystems for mitigation of the turbulence and background effects in the telescope arrays-based receivers, operating in a deep-space optical communication link. The analysis is based upon the MLCD proposal specifications for an optical communication link with planet Mars. Pulse-position modulations (PPM) along with the direct-detection techniques are employed. A Poisson probability model is used to calculate the signal and background photons. The analysis shows that the use of AO systems significantly improves the performance of the direct-detection array receivers. The paper is organized as follows. The origin and nature of atmospheric turbulence is discussed in Section 2. Telescope array receiver concept is explained in Section 3. Details of MLCD specifications are delineated in Section 4. Details of AO subsystems are given in Section 5. Monte Carlo simulation results are discussed in Section 6, and finally conclusions are made in Section 7.

## II. ORIGIN OF ATMOSPHERIC TURBULENCE

Atmospheric turbulence, generated by the pressure and temperature differentials in the atmosphere, creates fluctuations in the atmosphere's refractive index called the *optical turbulence*. Optical turbulence results in beam wander, a random redistribution of the beam energy within the cross section of beam leading to irradiance fluctuations, and a loss of spatial coherence of laser beam as it propagates through the atmosphere [14, 15]. Use of relatively large aperture receivers ( $D \approx 0.5\text{-m}$  and above) reduces the irradiance fluctuations and scintillations through aperture averaging [16]. However, the loss of spatial coherence limits the extent of focusing capabilities of the collecting aperture. As a result, the point spread function (PSF) deviates from the ideal diffraction limited performance. In the diffraction-limited case, the incoming plane waves from a distant point source is focused into a spot size, limited only by the size of the collecting aperture, i.e.,  $\approx(2.44\lambda/D)$ . In this regime, the background noise is not dependent upon the aperture size. Hence, the aperture size can be increased to increase the signal to background ratio photons. However, In the presence of turbulence, the focused spot size is limited by the atmospheric Fried parameter  $r_o$  (which varies from 20-cm to 4-cm with the turbulence strength), i.e.,  $\approx(\lambda/r_o)$ . In this regime, to capture the same amount of signal as that of diffraction limited case, we need to increase the detector area. However, we cannot increase the detector sizes because of two severe problems. First, increasing the detector size increases the background noise. Secondly, a large detector has a larger capacitance and smaller bandwidth.

The behavior of a sub portion of optical turbulence can be described in a statistical manner, and forms the basis of most

propagation theories. For optical wave propagation, the associated power spectral density for refractive index fluctuations can be described by von Karman spectrum [16],

$$\Phi_n(\kappa) = 0.033 C_n^2 \exp(-\kappa^2 / \kappa_m^2) / (\kappa^2 + \kappa_o^2)^{11/6}, \quad 0 \leq \kappa \leq \infty \quad (1)$$

where  $\kappa$  is the spatial frequency in the telescope aperture plane,  $\kappa_0 = 2\pi/L_o$ ,  $\kappa_m = 5.92/l_o$ ,  $L_o$  and  $l_o$  are outer and inner scales, respectively. The atmospheric turbulence effects are simulated by generating a phase screen on the telescope aperture by using the methods described in [17, 18]. The aperture plane signal distribution is Fourier transformed to get the focal-plane intensity distribution of the received signal. An example of the simulated turbulence effects for a telescope with  $D = 1\text{-m}$  and  $r_o = 4\text{-cm}$  is shown in Fig. 1. The aperture plane phase distribution in Fig. 1(a) clearly deviates from the ideal plane wave. Fig. 1(b) shows the focal-plane distribution.

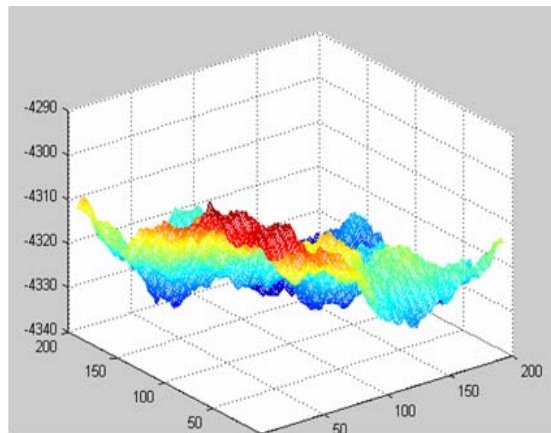


Fig. 1(a)

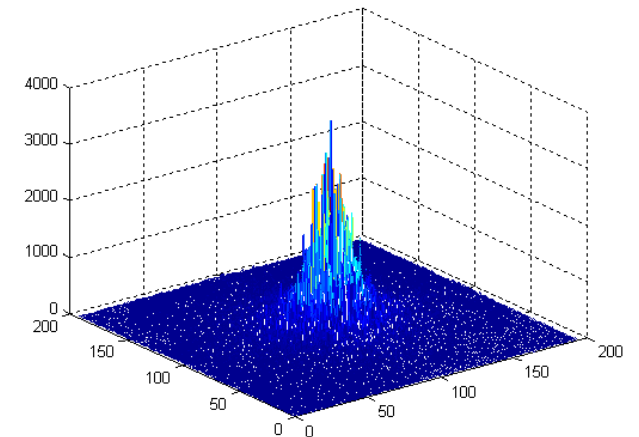


Fig. 1(b)

Fig. 1. (a) Phase distribution on an aperture of  $D = 1\text{-m}$  and Fried parameter  $r_o = 4\text{-cm}$ , (b) corresponding focal plane distribution.

### III. TELESCOPE ARRAY RECEIVER

A telescope acts as an antenna in an optical communication link. The telescope focuses the incoming light fields onto the photodetectors in the focal-plane. The photodetectors perform the optical to electrical signal conversion followed by the receiver electronics. A telescope array receiver is an aggregation of a number of relatively small-sized telescopes connected to form a larger total photon-collecting area. The number and size of the telescopes is selected so that the collective aperture of the array gives the same combined gain as that of a single large telescope. The performance of the array is theoretically similar to a single large telescope as long as the telescope diameter exceeds that of the coherence length of the atmosphere [10, 11]. Conceptual design of the telescope array receiver is shown in Fig. 2. Each telescope collects a portion of the incoming optical beam and focuses the energy onto its detectors. Each telescope has individual photodetectors, photon counters, front-end optical filter, clock and fast steering mirror based closed-loop tracking subsystem. AO subsystems are employed in each telescope to compensate for turbulence effects. Detected signals after AO correction from all the telescopes are sent to a central combining unit via high-speed digital network. Central combining unit combines the signals from all the telescopes after delay compensation and synchronization. The combined signal is sent to the digital decoder for data extraction and information recovery. The vital concept in a telescope array is that the signals are first phase corrected by the AO systems, optically detected at different array elements, and then combined afterwards for the decoding purposes.

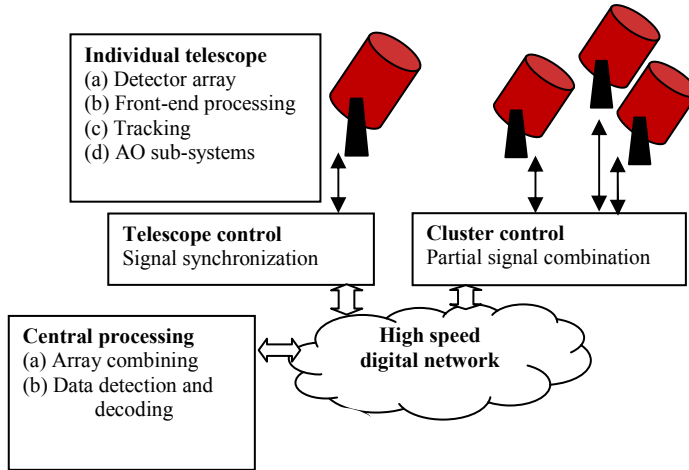


Fig. 2. Conceptual design of an AO based telescope array receiver.

### IV. MLCD MISSION

Mars Laser Communication Demonstration (MLCD) mission was announced to test the first-ever interplanetary laser-communication link between Earth and Mars in the 2009-2011 time frame [6]. A practical approach is to base the system analysis around this realistic mission. Hence, the MLCD system specifications are used as the baseline platform for the simulations and evaluation of the optical receivers in this paper. According to MLCD initial plans

[7], the flight terminal has a 30-cm. diameter, near diffraction-limited telescope with a linear obscuration of 10 % that transmits a pulse-position modulated (PPM) signal, at a wavelength of  $1.06\mu\text{m}$ , and an average power of 5W.

The available link capacity during satellite orbit around Mars varies an order of magnitude due to variations in distance, background noise, and atmosphere turbulence [19]. Table 1 shows the range of link parameter variations for a typical Mars to Earth communication link [19].

Table 1. Link budget parameters for optical communication link between a spacecraft in Mars orbit and an Earth-based receiver, based upon MLCD proposal.

Parameter	Min.	Max.	Selected
Transmitter power (W)	5.0	5.0	5.0
Peak power (W)	$3.2 \times 10^2$	$1.3 \times 10^3$	Variable
Path loss (dB)	361.5	372.47	372.47
Transmitter telescope gain (dB)	115.7	118.1	117.0
Transmitter loss (dB)	1.43	2.34	1.43
Receiver loss (dB)	4.58	5.58	4.58
Pointing loss (dB)	1.25	2.0	1.25
Background loss(dB)	5.3	8.38	5.3
Background noise density ( $\text{SEP} = 3^\circ$ ) $\mu\text{W} / (\text{cm}^2 - \text{sr} - \text{nm})$	2	100	Variable
Optical filter bandwidth, nm	0.1	0.1	0.1

### V. ADAPTIVE OPTICS (AO) SYSTEMS

An AO system includes three basic elements, a wavefront sensor, a deformable element, and a feedback scheme. Typically, these components are a Shack-Hartmann sensor, a bimorph or segmented mirror, and PC-based software for performing the necessary calculations and controlling the deformable mirror. The block diagram of the AO system is given in Fig. 3.

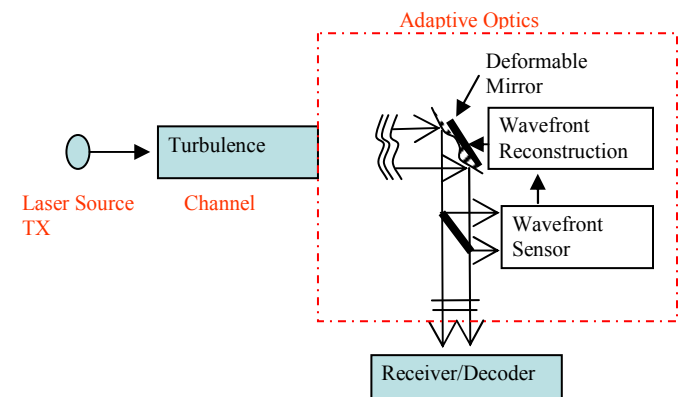


Fig. 3. Block diagram of an AO system.

The wavefront sensor calculates the wavefront distortions.

The feedback control-loop controls the deformable mirror, applies the conjugate of phase error to the distorted wavefront and compensates for the turbulence distortions. After the correction, the received pattern approaches the ideal Airy disc, and a smaller detector is used in the focal-plane, thus spatially rejecting the most of background noise fields.

Since the received signal power is not enough to estimate and correct the phase front error, a laser guide star (LGS) based AO system is used. Although adding LGS AO system for each telescope in an array increases the cost, but this added cost can be justified with the overall cost reduction due to a decrease in the required photon-collecting area. Performance of a LGS-based AO system depends on various parameters and requires careful design to achieve the optimum performance. This performance corresponds to the remaining wavefront error after wavefront correction [20,21]. The efficiency of the Adaptive optics system error is represented by the Strehl Ratio (SR) of the system after phase correction, which is the ratio of the maximum power density in the focal-plane of actual system to that in the diffraction-limited system. We will incorporate and evaluate AO systems with different complexities (i.e., SR = 0.3 and SR = 0.8) to find the impact on the deep-space optical link.

## VI. PERFORMANCE ANALYSIS OF AO SUBSYSTEM BASED TELESCOPE ARRAY RECEIVER

In this section, we investigate the performance of an AO based telescope array receiver for a deep-space optical communication link with Mars, based upon MLCD specifications. It is well-established in the literature that  $M$ -ary pulse-position modulation (PPM) is a practical and optimal modulation format to achieve high peak-to-average-power ratio in a deep-space optical link [22, 23], and most deep-space optical links analyzed to date had assumed  $M$ -ary PPM modulations [3]. Hence, PPM scheme along with the direct detection optical receiver is employed in the simulations.

### A. Communication system model

In the  $M$ -ary optical pulse-position modulation (PPM) technique [23], digital data is encoded by the position of an optical pulse slot within a frame of  $M$  possible slots. The performance of the receiver depends on the PPM order  $M$ , received signal and background noise photons, and other limiting factors such as, atmospheric turbulence, receiver internal noise, as well as synchronization and tracking losses.

#### 1) Received Signal photons model

The number of signal photons received at the receiver is a function of transmitter, receiver, and channel parameters. Assuming ideal conditions, the average received signal photons count  $K_s$  per signal slot at wavelength  $\lambda$  over a link distance  $L$  is given by

$$K_s = P_r G_r \eta_r G_s \eta_s \eta_{atm} \left( \frac{\lambda}{4\pi L} \right)^2 M T_s \left( \frac{\eta_{det}}{hc} \right), \quad (2)$$

where  $P_r$  is the average transmitted power;  $\eta_r, \eta_s, \eta_{atm}$  are the transmitter, receiver, and atmospheric efficiencies at the

optical wavelength  $\lambda$ , respectively;  $T_s$  is the slot width and  $M T_s$  represents the PPM frame length;  $\eta_{det}$  is the detector quantum efficiency and  $hc/\lambda$  is the single photon energy at the carrier frequency.  $G_r$  and  $G_s$  are the transmitting and receiving antenna gains, respectively.

#### 2) Received Background photons model

The background light in deep-space optical links arises from extended sources like diffuse light from the Sun, sky, etc. during day time and point sources like stars, planets during the night time. Background light fields enter the optical receiver from all directions, and appear as a spatially flat intensity distribution, uniformly spread over the detector surface effectively adding a spatial noise flow to the focused source signal field. The total background power is given by [24]

$$P_b = P_{bo} \left( \frac{\Omega_{fi}}{\Omega_{dl}} \right) \quad (3)$$

where

$$P_{bo} = L(\lambda)(\Delta\lambda)\lambda^2 \quad (4)$$

is the diffraction-limited power per spatial mode and  $\Omega_{fi}/\Omega_{dl}$  is the number of turbulence-induced random modes observed by the optical receiver.  $L(\lambda)$  is the spectral irradiance of the background source,  $\Delta\lambda$  is the optical bandwidth,  $\Omega_{fi}$  is the actual receiver field of view, and  $\Omega_{dl}$  is the diffraction-limited field of view.

#### 3) Performance of the optical direct-detection PPM receiver

Performance of the receiver is described in terms of the capacity of the link. The link capacity depends on the bit-error rate (BER), which is a function of the average received signal and background photons, and PPM order  $M$ .

According to the Maximum Likelihood (ML) detection strategy, the probability of correct detection  $P_c$  for a Poisson channel is given by [24].

$$\begin{aligned} P_c = & \frac{\exp[-(K_s + MK_b)]}{M} - \\ & \sum_{k_1=1}^{\infty} Pos(k_1, K_s + K_b) \left[ \sum_{k_2=1}^{k_1-1} Pos(k_2, K_b) \right]^{M-1} - \\ & \sum_{r=1}^{M-1} \frac{(M-1)!}{r!(M-1-r)!(r+1)} \sum_{k=1}^{\infty} Pos(k, K_s + K_b) [Pos(k, K_b)]^r \times \\ & [\sum_{j=0}^{k-1} Pos(j, K_b)]^{M-1-r}, \end{aligned} \quad (5)$$

and the probability of error  $P_e$  can be written as  $P_e = 1 - P_c$ .

The capacity of an  $M$ -ary symmetric Poisson channel depends upon the symbol-error-rate (SER), is given by [3]

$$C = \log_2 M + p \log_2 p + q \log_2 \left( \frac{q}{M-1} \right) \text{ bits/symbol} \quad (6)$$

where  $p$  is the probability of correct symbol detection  $q$  and is the SER.

### B. Monte Carlo simulations

In this section, we investigate the achievable data rates versus different receiver telescope aperture sizes, for different AO systems. Monte Carlo simulations of an end-to-end optical communication link between Earth and Mars are carried out according to MLCD specifications. The link is tested for the most difficult scenario, i.e. when Mars is at the farthest distance from Earth (conjunction), and background noise is at its peak, i.e.,  $L = 100 \mu\text{w}/(\text{cm}^2 - \text{str} - \text{nm})$ . The parameters shown as “selected” in Table 1 are used for rest of the link-budget calculations. The signal and background photons are calculated according to the model described in previous sections. In this analysis,  $M = 256$  PPM and a detector with quantum efficiency  $QE = 0.45$  is assumed. In addition, detector diameter and PPM slot durations are optimized to obtain maximum achievable bit-rates. Von Karman model for atmospheric turbulence is employed. The main design parameters of the array architecture are the sizes of the individual telescopes and the number of telescopes in the array. However, the total photon-collecting aperture of the complete telescope array receiver remains constant in each case for uniformity in comparison. We start with a monolithic large telescope of 10-m diameter, i.e. the  $(1 \times 10\text{m})$  configuration. Then, we increase the number of telescopes in the array by breaking down the single aperture into 4, 16, 100, and 135 elements of 5-m, 2.5-m, 1-m, and 0.86-m telescope aperture diameters, respectively, i.e.,  $(4 \times 5\text{m})$ ,  $(16 \times 2.5\text{m})$ ,  $(100 \times 1\text{m})$ , and  $(135 \times 0.86\text{m})$  configurations. The parameters used in the simulations and the channel capacity results are given in the Table 2. The achievable data rates are given in Figure 5. The figure shows that as we increase the array dimensionality, i.e., increase the number of telescope elements in the array receiver from 1 to 135, the link capacity deteriorates by a negligible amount. Hence, it is feasible to employ the telescope arrays-based receiver instead of a single, large, and costly telescope.

The figure also shows that the use of AO system results in considerable improvement in data rates. Without the AO system, the achievable data rates are in the range of 1 M bits/sec. However, with an AO system achieving SR = 0.3, the data rates increase to 5 M bits/sec. As we increase the complexity of the AO systems and achieve SR = 0.8, the data rates of 12 M bits/sec are possible with an array of 100 smaller telescopes. The employment of actual AO system in an actual receiver will be driven by the cost variables. However, it is important to highlight that AO systems for the smaller telescopes in the array are much cheaper, as less actuators are required in deformable mirrors. Hence, our results not only demonstrate the large gains in the achievable channel capacity made possible by incorporating the AO systems, but also solidify the feasibility analysis of telescope arrays-based optical receivers for deep-space optical communication links.

### VII. CONCLUSION

We simulated and evaluated an AO based telescope array-based receiver for deep-space optical communications link with Mars in most difficult channel conditions. Data rates of up to 13 m bits/sec are possible with an AO system achieving SR=0.8, which are orders of magnitude greater than the current achievable data rates by the RF-based NASA DSN receivers during the similar channel conditions. Hence, AO based optical arrays is a viable option for fulfilling the large bandwidth demands of future deep-space exploration missions.

### REFERENCES

- [1] W. J. Weber, R. J. Cesare, D. S. Abraham, P. E. Doms, R. J. Doyle, C. D. Edwards, J. Hooke, J. R. Lesh, and R. B. Miller, “Transforming the deep space network into the interplanetary network,” Paper IAC-03-U.4.01 *54th International Astronautical Congress*, Bremen, Germany, 2003.
- [2] J. Taylor, M. Muñoz Fernández, A. B. Alamanac, and Kar-Ming Cheung, “Deep Space 1 Telecommunications.” *Design and Performance Summary Series*, Deep Space Communications and Navigation Systems Center of Excellence (DESCANSO), Jet Propulsion Laboratory, California Institute of Technology, Pasadena, CA, U.S.A.
- [3] H. Hemmati (Editor), “*Deep Space Optical Communications*,” New Jersey: John Wiley and Sons, 2006.
- [4] J. Taylor et al., “Mars Exploration Rover Telecommunications.” *Design and Performance Summary Series*, Deep Space Communications and Navigation Systems Center of Excellence (DESCANSO), Jet Propulsion Laboratory, California Institute of Technology, Pasadena, CA, U.S.A, 2005.
- [5] National Aeronautics and Space Administration 2003 Strategic Plan, 2003.
- [6] B. L. Edwards, et al., “Overview of the Mars Laser Communications Demonstration Project,” Paper 2003-6417, *AIAA Space 2003 Conference*, Long Beach, California, September 23–25, 2003.
- [7] D. M. Boroson, A. Biswas, and B. L. Edwards, “MCLE: Overview of NASA’s Mars laser communication demonstration system”, In *Proc. SPIE*, vol. 4635, 2004, pp. 16-28.
- [8] K. E. Wilson, N. Page, J. Wu, and M. Srinivasan, “The JPL optical communications telescope laboratory test bed for the future optical deep space network”, *IPN Progress Report 42-153*, May, 2003.
- [9] M. Britcliffe, D. Hoppe, W. Roberts, and N. Page, “A 10-m ground-station telescope for deep-space optical communication: A preliminary design,” in *IPN Progress Report 42-147*, Nov., 2001.
- [10] A.A.Eftekhar, S. Khjorasan, A. Adibi, F. Amoozegar, and S. Piazolla, “Analysis of telescope arrays for deep space optical communications”. *Proc. IEEE Aerospace conference*, 2005. pp. 1589-1597.
- [11] V. A. Vnlrotter, C. W. Lau, M. Srinivasav, K. Andrews, and R. V. Mukai, “Optical array receiver for communication through atmospheric turbulence”. *Journal of Lightwave Technology*, vol. 23, no. 4, Apr., pp. 1664-1675, 2005.
- [12] L.C. Andrews and R.L. Phillips, “*Laser beam Propagation through Random Media*,” SPIE Press, Bellingham, Washington, 2005.
- [13] V. A. Vnlrotter, Background sources in optical communications, *JPL Publication 83-72*, Jet Propulsion Laboratory, Pasadena, California, November 15, 1983.
- [14] I. Tatarski, “*Wave Propagation in A Turbulent Medium*,” McGraw-Hill, New York, translated by R. A. Silverman, 1961.
- [15] A. Ishimaru, “*Wave Propagation and Scattering in Random Media*,” IEEE Press, Piscataway, New Jersey, 1997.
- [16] L. C. Andrews and R. L. Phillips, “*Laser Beam Propagation through Random Media*,” SPIE Optical Engineering Press, Bellingham, Washington, pp. 157–229, 1998.
- [17] B.L. McGlamery, “ Computer simulation studies of compensation of turbulence degraded images,” In *Proc. SPIE* 74, 1976, pp. 225-233.
- [18] P.N. Regagnon, “ Practical aspects of image recovery by means of the bi-spectrum” *J. Opt. Soc. Am A.* , vol. 13, no. 7, July 1996.

- [19] A. Biswas, S. Piazzolla , "Deep space optical communications downlink budget from Mars : System parameters," in *IPN Progress Report* , August 2003.
- [20] Truong et al., "Real-time wavefront processors for the next generation of adaptive optics Systems: A design and analysis," In *Proc. SPIE*, vol. 4839, 2003, pp. 911–922.
- [21] M.A.van Dam and B. A. Macintosh, "Characterization of adaptive optics at Keck observatory," In *Proc. SPIE*, vol. 5169, 2003, pp. 1–10.
- [22] J. R. Lesh, "Capacity limit of the noiseless, energy-efficient optical PPM channel," *IEEE Transactions on Communications*, vol. COMM-31, no. 4, pp. 546–548, 1983.
- [23] D. Zwillinger, "Maximizing throughput over an average-power-limited and band-limited optical pulse-position modulation channel," *The Telecommunication and data Acquisition Progress Report 42-62, January and February 1981*, Jet Propulsion Laboratory, Pasadena, California, pp. 81-86, April 15, 1981.
- [24] R.M. Gagliardi and S. Karp, *Optical Communications*, 2<sup>nd</sup> ed., New York: John Wiley and Sons, 1995.

Table 2. Maximum achievable data rates from telescope arrays with different array architectures.  $N$  is the number of telescopes in array, SR is the Strehl ratio and represents the amount of correction by AO system.  $r$  is the detector size normalized with respect to the diffraction-limited spot size

$N \times D$ (m)	$r_o$ (m)	$M$	SR	$n_{p_0}$ photon/ ns/m <sup>2</sup>	$n_{b_0}$ photon/ ns	$\tau$ ns	$r$ (1/ $\lambda$ F)	<b>Bit rate</b> M Bit/s
$1 \times 10$	0.04	256	0.3	0.0947	7.39e-4	2	1.81	7.91
$16 \times 2.5$	0.04	256	0.3	0.0947	7.39e-4	2	1.81	6.94
$100 \times 1$	0.04	256	0.3	0.0947	7.39e-4	3	1.51	4.96
$135 \times 0.86$	0.04	256	0.3	0.0947	7.39e-4	3	1.51	4.49
$1 \times 10$	0.04	256	0.8	0.0947	7.39e-4	2	1.81	14.03
$16 \times 2.5$	0.04	256	0.8	0.0947	7.39e-4	2	1.81	13.65
$100 \times 1$	0.04	256	0.8	0.0947	7.39e-4	2	1.51	12.44
$135 \times 0.86$	0.04	256	0.8	0.0947	7.39e-4	2	1.51	12.04

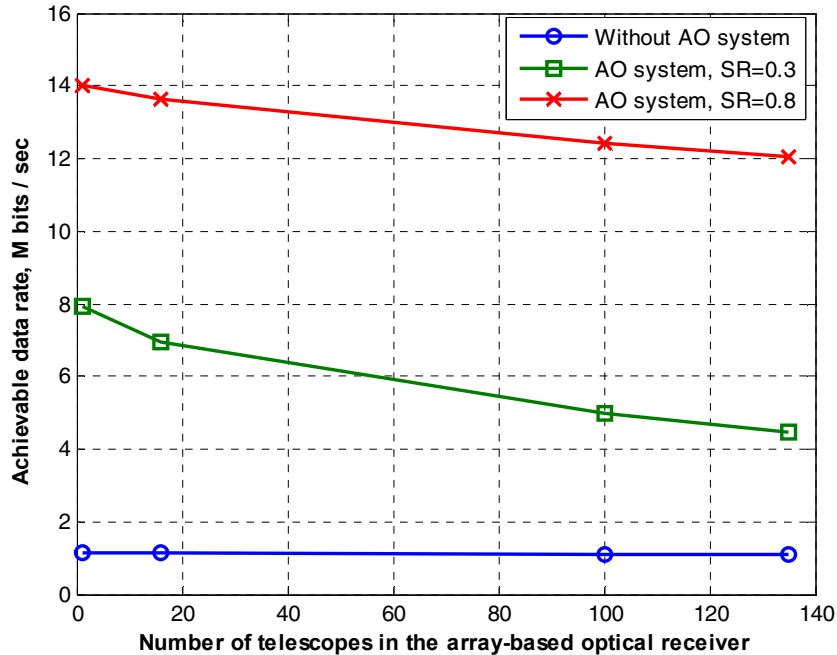


Fig. 5. Achievable data rates vs. different array architectures, for different AO systems with varying complexities.